RAI Volume 3, Chapter 2.2.1.3.6, First Set, Number 6, Supplemental Questions:

1. As stated in the response to RAI 3.2.2.1.3.6-006, an alternative representation (Case 6c) of flow focusing leads to an increase in mean seepage rate by a factor of 3.3 compared to the nominal distribution of flow focusing.

   a. What is the answer to the second part of the RAI, i.e., what is the performance consequence of this factor increase?

   b. Describe the distribution (mathematically) and the basis for the flow focusing factor for Case 6c, which is possibly the same as used in *Abstraction of Drift Seepage*, MDL-NBS-HS-000019 REV 1, AD 01, Section 6.8.2, Case 6.

2. Describe why performance is insensitive to seepage fraction.

   Section 1.4.2 of the DOE response to RAI 3.2.2.1.3.6-006 describes repository performance as insensitive to seepage fraction. Also, SAR Section 2.3.3.2.3.4.1 similarly describes a lack of sensitivity of performance to seepage fraction changes caused by increased waste package length. Given the insensitivity for performance, how does the decrease in seepage fraction for Case 6c offset the seepage increase (see Section 1.4.1 of the DOE response)?

1. SUPPLEMENTAL RESPONSE

This supplemental response presents the mathematical basis for the extreme-bounding distribution for flow focusing (referred to as Case 6c in the response to RAI 3.2.2.1.3.6-006) in Section 1.1 and Appendix A and explains why the case is useful in understanding the system sensitivities to flow focusing but is not a realistic representation of the physical system. A total system performance assessment (TSPA) sensitivity analysis using the Case 6c distribution for flow focusing instead of the base case flow focusing distribution described in Section 1.2 demonstrates the hypothetical performance consequence of using Case 6c. The performance consequence associated with using the Case 6c flow focusing factor to derive seepage rates and seepage fractions is relatively small, as discussed in Section 1.2. The seismic ground motion modeling case, which is one of the two modeling cases that are major contributors to dose for the 1,000,000-year analysis, has a mean annual dose increase of 0.32 mrem, or 28%, resulting from the increase in mean seepage rates and decrease in seepage fractions associated with the use of the alternative flow focusing factor distribution. An increase in expected annual dose of approximately 0.32 mrem with respect to a base case value of 2.00 mrem represents a minor effect. Note that the other modeling case that has a major impact on dose, the igneous intrusion modeling case, does not consider flow focusing in its seepage calculations. A discussion of performance insensitivity to seepage fraction is presented at the end of Section 1.2.

1.1 MATHEMATICAL BASIS FOR THE CASE 6c DISTRIBUTION

The alternative flow focusing distribution referred to in Case 6c (SNL 2007a, Section 6.8.2) was derived from the base case distribution by applying a cubic transformation to the flow focusing factor, and then normalizing the distribution such that the mean flow focusing factor has a value of 1. Normalizing the distribution such that the mean flow focusing factor has a value of 1 prevents biasing the sampling towards an average percolation rate through the repository footprint of greater than the unfocused average rate (mean flow focusing factor > 1) or less than the unfocused average rate (mean flow focusing factor < 1). This process leads to a flow focusing distribution with a maximum flow focusing factor of about 33, as compared with a maximum value of about five for the base case distribution. Mathematically, the alternative flow focusing distribution (Case 6c) is:

$$Y = -1.826X^{4/3} + 20.61X - 86.04X^{2/3} + 158.9X^{1/3} - 11.434 \qquad \text{(Eq. 1)}$$

where Y is the cumulative probability expressed as a percentage and X is the flow focusing factor (see Appendix A of this response, for the derivation).

The flow focusing distributions for the base case and Case 6c are compared in Figure 1. When such distributions are manipulated to extend the range of focusing factors that are greater than 1, but are constrained to maintain a mean of 1, the frequency of focusing factors less than 1 must also increase. As shown in Figure 1, the probability of a flow focusing factor less than 1 is 60% in the base case as compared to 80% in Case 6c.

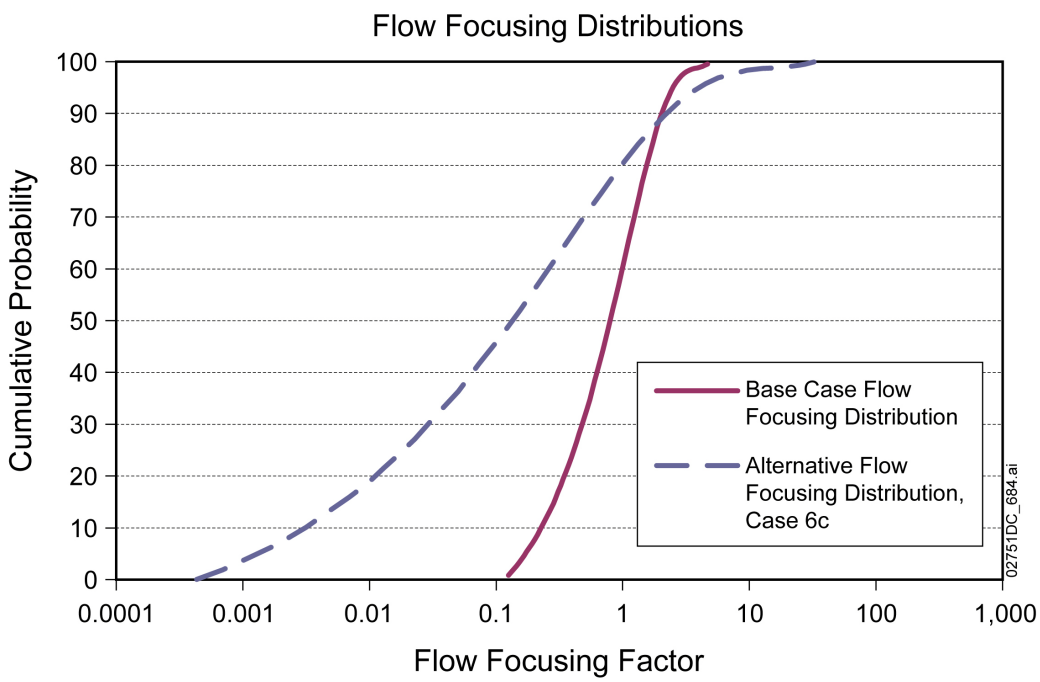

Source: Equation 1 of this response, and the "Previous" distribution from SNL 2007a, Figure 6.6-15.

Figure 1. Comparison of Base Case and Alternative (Case 6c) Cumulative Flow Focusing Distributions

In a previous version (REV 01) of *Abstraction of Drift Seepage*, flow focusing distributions based on active fracture spacing were derived. The method used to derive these flow focusing distributions assumed that flowing fractures were saturated, which is equivalent to assuming that the active fracture parameter γ has a value of 1. Using the assumption of saturated flowing fractures, the derived distributions were found to have maximum flow focusing factors of 9.7, 22, and 47 for different glacial-transition infiltration cases. However, note that an active fracture parameter of 1 is inconsistent with the calibrations to water saturation and water potential (SNL 2007b, Section 6.3.2) and with validations against carbon-14 and calcite coating data (BSC 2004, Sections 7.4.1 and 7.4.2). These calibrations and validations indicate that the active fracture parameter is on the order of 0.4 or lower.

The maximum flow focusing factor, 33, for Case 6c lies within the range of the three distributions discussed above. The distribution function for Case 6c (Equation 1) was developed as a representation of such broad focusing distributions for use in the sensitivity analysis (SNL 2007a, Section 6.8.2). The base case flow focusing factor distribution is derived from a process-level description of unsaturated flow representing the effects of small- to intermediate-scale heterogeneity in fracture permeability. By comparison, the flow focusing distribution developed previously as discussed above is a less direct method to estimate flow focusing. Therefore, the alternative flow focusing distribution used in Case 6c is only suitable to investigate the sensitivity of the seepage abstraction to flow focusing, and is not representative of the physical system.

1.2 TSPA SENSITIVITY ANALYSIS USING THE CASE 6c DISTRIBUTION AND THE RESULTING PERFORMANCE CONSEQUENCE

As noted in DOE's response to RAI 3.2.2.1.3.6-006, Case 6c is an extreme case that was developed only to illustrate the extent to which seepage rates might vary for different distributions of the flow focusing factor. Case 6c is not representative of the physical system as discussed above, and accordingly, the original response to RAI 3.2.2.1.3.6-006 did not directly address the performance consequence that would be simulated if this distribution were used in TSPA.

For this supplemental response, the performance consequence that would result from using Case 6c is determined. Only the 1,000,000-year seismic ground motion modeling case is considered, because this modeling case and the igneous intrusion modeling case together control the total mean annual dose results (SNL 2008, Figure 8.1-3b[a]). Also, flow focusing and capillary diversion, in representing the flow of water that interacts with failed waste packages, are inapplicable to the igneous intrusion modeling case. The mean of the expected annual dose that results from using the Case 6c flow focusing distribution (Equation 1 and Appendix A, herein) is compared to the results from a correction to the base case. The uncorrected mean of the base case results is presented in the TSPA report (SNL 2008, Figure 8.1-2[a]), which used the base case flow focusing factor distribution (SNL 2007a, Section 6.7.1.1). The following discussion describes the correction, which was in response to an error discovered in the generation of seepage rates in the TSPA, and then presents the simulation results (Table 1, Table 2, Figures 3 and 4).

This response compares results for the base case TSPA model, which uses the seepage software *SEEPAGEDLL_LA.dll*, with results obtained for the base case focusing using a corrected version of the seepage software. The corrected base case is then compared to the Case 6c simulation, which was generated using the corrected version of the seepage software, with the alternative flow focusing factor implemented. The correction fixes an error in applying an upper limit for seepage rates. The error affects the upper bound of the calculated final seepage rate for individual waste package locations. In the seepage software used in the TSPA model, the seepage rate for each location is first interpolated from a look-up table using the local percolation flux, the log-permeability, and the capillary strength. The local percolation flux is defined as the product of the percolation flux, at a waste package location, and a flow focusing factor that accounts for intermediate-scale permeability variability above the drift (SNL 2007a, Section 6.7.1.1). The interpolated seepage rate is then adjusted for seepage model uncertainty to obtain the final seepage rate. If the final seepage rate (after adjustment for seepage model uncertainty) is greater than the volumetric flow from the local percolation flux impinging on the drift opening over an average waste package, the seepage software is supposed to set the final seepage rate for the individual waste package location equal to a value based on the local percolation flux (which is the product of the percolation rate at a specific waste package location and the sampled flow focusing factor). However, in the seepage software version used for TSPA, the calculated final seepage rate was incorrectly compared to a volumetric flow rate that was computed using the percolation flux, rather than with a volumetric flow rate computed using the local percolation flux (i.e., percolation flux multiplied by the flow focusing factor). This error occurred infrequently, and tended to generate lower spatially-averaged seepage rates in all TSPA scenario classes that use the seepage abstraction (i.e., all scenario classes except the igneous scenario class). The imperceptible effect of correcting the software error on mean annual dose calculations is shown in Figure 2, which compares the results from the TSPA base case with results generated using a corrected version of the seepage software.

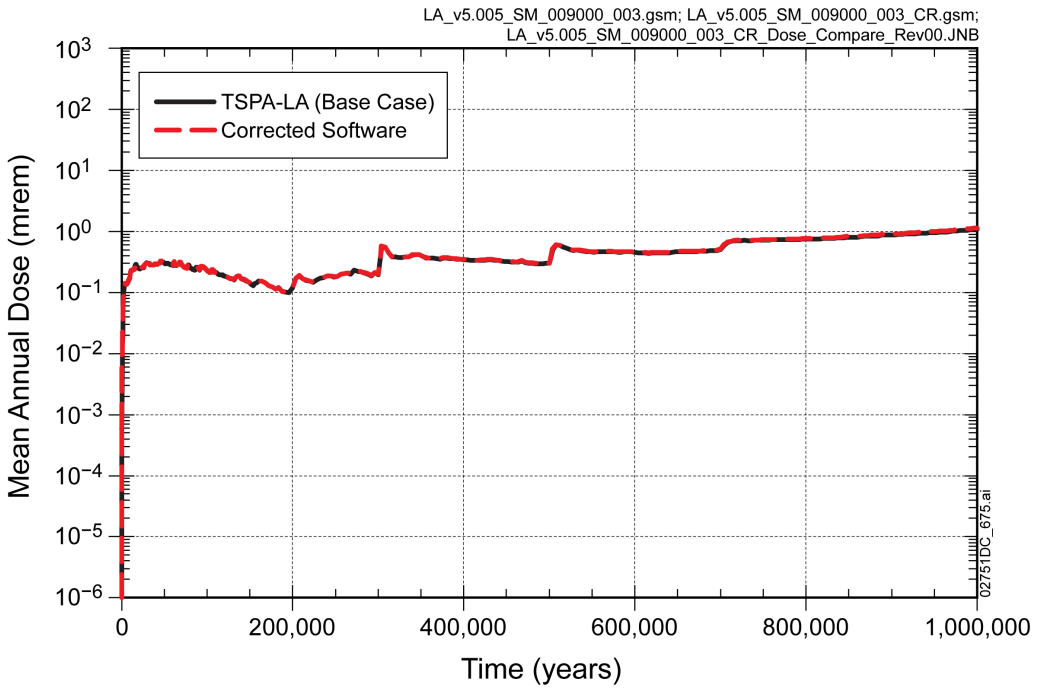

Figure 2. Comparison of Base Case TSPA Mean Annual Dose Results for the 1,000,000 Year Seismic Ground Motion Modeling Case, with Results Using Corrected Seepage Software

Tables 1 through 4 contain a breakdown of the volumetric seepage rates for commercial spent nuclear fuel (SNF) and codisposal waste packages by infiltration case (based on the 10th, 30th, 50th, and 90th percentile infiltration maps), climate states, and percolation subregions, for base case flow focusing (Table 1 for commercial SNF and Table 2 codisposal waste packages) and Case 6c flow focusing (Table 3 for commercial SNF and Table 4 for codisposal waste packages). The results presented in Tables 1 and 2 were generated using the corrected version of the TSPA seepage software. The results presented in Tables 3 and 4 were generated using the corrected version of the TSPA seepage software changed to include the Case 6c flow focusing factor. The seepage results for the three climate states (present-day, monsoonal, glacial-transition) and the post-10,000-year climate change are determined at 500, 750, 10,000, and 1,000,000 years, respectively. The effect of correcting the error in the seepage software can be determined by comparing Tables 1 and 2 of this response with Tables 9 and 10 in the response to RAI 3.2.2.1.3.6-005 on seepage rates. A comparison between Table 1 of this response and Table 9 in the response to RAI 3.2.2.1.3.6-005 reveals that the average seepage rate for the glacial-transition climate increased 21% after correction of the implementation error. For the post-10,000-year climate state, the average seepage rate increased 14%. Similar increases were seen for the codisposal waste packages (Table 2 of this response and Table 10 in the response to RAI 3.2.2.1.3.6-005). As can be seen by comparing Table 1 of this response and Table 9 in the response to RAI 3.2.2.1.3.6-005, the seepage fractions are not affected by the error. Seepage results for commercial SNF waste packages presented in Tables 1 and 3 (and seepage results for codisposal waste packages presented in Tables 2 and 4) demonstrate that when the Case 6c flow focusing distribution is used, the mean seepage rate increases and mean seepage fraction (i.e., fraction of waste package locations with seepage) decreases.

Table 1. Average Seepage Rates and Fractions for the Corrected Seismic Ground Motion Modeling Case for Commercial SNF Waste Packages (Base Case Flow Focusing; Results for Seeping Environments Only)

Infiltration Map Percentile[a]	Climate State	Average Rate over the Subregion (m^3/yr per WP)[b]					Repository Average (m^3/yr per waste package)
		1	2	3	4	5	
		0.05[c]	0.25[c]	0.4[c]	0.25[c]	0.05[c]	
10th *p*= 0.6191	Present-Day	0.0001	0.0008	0.0014	0.0017	0.0035	0.0014
	Monsoon	0.0008	0.0063	0.0092	0.0097	0.0165	0.0086
	Glacial-Transition	0.0012	0.0050	0.0240	0.0603	0.1282	0.0324
	Post-10,000-year	0.0850	0.3348	0.4563	0.4703	0.5971	0.4179
	Seepage Fraction	0.442	0.608	0.667	0.639	0.694	0.635
30th *p*= 0.1568	Present-Day	0.0009	0.0077	0.0109	0.0131	0.0222	0.0107
	Monsoon	0.0035	0.0268	0.0398	0.0455	0.0649	0.0374
	Glacial-Transition	0.0079	0.0513	0.1192	0.1716	0.2624	0.1169
	Post-10,000-year	0.0726	0.3550	0.8997	1.3820	1.9248	0.8940
	Seepage Fraction	0.487	0.682	0.788	0.803	0.844	0.753
50th *p*= 0.1645	Present-Day	0.0018	0.0164	0.0221	0.0234	0.0416	0.0209
	Monsoon	0.0024	0.0265	0.0551	0.0676	0.1266	0.0520
	Glacial-Transition	0.0055	0.0532	0.1733	0.2844	0.4542	0.1767
	Post-10,000-year	0.1280	0.6710	1.2525	1.5947	2.0555	1.1766
	Seepage Fraction	0.503	0.718	0.799	0.797	0.833	0.765
90th *p*= 0.0596	Present-Day	0.0097	0.0766	0.1087	0.1079	0.1636	0.0983
	Monsoon	0.0673	0.4637	0.7034	0.7351	0.9902	0.6340
	Glacial-Transition	0.0208	0.2218	0.4745	0.5774	0.8417	0.4327
	Post-10,000-year	0.2315	0.9423	1.3909	1.5488	1.9069	1.2861
	Seepage Fraction	0.584	0.800	0.864	0.861	0.886	0.834
TSPA Mean Results	Present-Day	0.0011	0.0090	0.0127	0.0134	0.0223	0.0118
	Monsoon	0.0055	0.0403	0.0631	0.0683	0.1005	0.0577
	Glacial-Transition	0.0042	0.0331	0.0903	0.1454	0.2453	0.0932
	Post-10,000-year	0.0989	0.4293	0.7119	0.8615	1.1219	0.6685
	Seepage Fraction	0.467	0.649	0.719	0.704	0.752	0.687

[a] GLUE probability weighting factors for the 10th, 30th, 50th, and 90th percentile infiltration realizations: SAR Section 2.3.2.4.1.2.4.5.5.

[b] Percolation subregions and quantile ranges: SAR Section 2.4.2.3.2.1.2.

[c] Fraction of waste packages in Percolation subregions.

NOTE: TSPA seepage data extracted at 500-, 750-, 10,000-, and 1,000,000-year time steps for the present-day, monsoon, glacial-transition, and post-10,000-year climate states, respectively.

Table 2. Average Seepage Rates and Fractions for the Corrected Seismic Ground Motion Modeling Case for Codisposal Waste Packages (Base Case Flow Focusing; Results for Seeping Environments Only)

Infiltration Map Percentile[a]	Climate State	Average Rate over the Subregion (m^3/yr per WP)[b]					Repository Average (m^3/yr per waste package)
		1	2	3	4	5	
		0.05[c]	0.25[c]	0.4[c]	0.25[c]	0.05[c]	
10th *p*= 0.6191	Present-Day	0.0001	0.0009	0.0017	0.0022	0.0040	0.0016
	Monsoon	0.0009	0.0064	0.0097	0.0105	0.0169	0.0090
	Glacial-Transition	0.0012	0.0050	0.0241	0.0607	0.1264	0.0324
	Post-10,000-year	0.0850	0.3324	0.4575	0.4706	0.5940	0.4177
	Seepage Fraction	0.440	0.608	0.667	0.641	0.697	0.636
30th *p*= 0.1568	Present-Day	0.0011	0.0088	0.0130	0.0154	0.0244	0.0125
	Monsoon	0.0033	0.0278	0.0416	0.0476	0.0645	0.0389
	Glacial-Transition	0.0078	0.0519	0.1198	0.1717	0.2571	0.1171
	Post-10,000-year	0.0736	0.3581	0.9076	1.3811	1.9241	0.8977
	Seepage Fraction	0.489	0.681	0.789	0.804	0.845	0.753
50th *p*= 0.1645	Present-Day	0.0024	0.0175	0.0264	0.0280	0.0472	0.0244
	Monsoon	0.0025	0.0257	0.0558	0.0680	0.1271	0.0522
	Glacial-Transition	0.0055	0.0520	0.1728	0.2785	0.4470	0.1744
	Post-10,000-year	0.1260	0.6673	1.2548	1.5746	2.0328	1.1703
	Seepage Fraction	0.504	0.715	0.800	0.798	0.828	0.765
90th *p*= 0.0596	Present-Day	0.0105	0.0796	0.1178	0.1140	0.1712	0.1046
	Monsoon	0.0651	0.4632	0.7023	0.7313	0.9901	0.6323
	Glacial-Transition	0.0199	0.2195	0.4713	0.5709	0.8372	0.4290
	Post-10,000-year	0.2324	0.9363	1.3864	1.5457	1.9014	1.2818
	Seepage Fraction	0.582	0.800	0.863	0.859	0.881	0.833
TSPA Mean Results	Present-Day	0.0013	0.0096	0.0145	0.0152	0.0243	0.0132
	Monsoon	0.0054	0.0403	0.0638	0.0690	0.1007	0.0582
	Glacial-Transition	0.0041	0.0329	0.0902	0.1443	0.2419	0.0927
	Post-10,000-year	0.0987	0.4274	0.7140	0.8581	1.1158	0.6677
	Seepage Fraction	0.467	0.648	0.720	0.705	0.753	0.687

[a] GLUE probability weighting factors for the 10th, 30th, 50th, and 90th percentile infiltration realizations: SAR Section 2.3.2.4.1.2.4.5.5.

[b] Percolation subregions and quantile ranges: SAR Section 2.4.2.3.2.1.2.

[c] Fraction of waste packages in Percolation subregions.

NOTE: TSPA seepage data extracted at 500-, 750-, 10,000-, and 1,000,000-year time steps for the present-day, monsoon, glacial-transition, and post-10,000-year climate states, respectively.

Table 3. Average Seepage Rates and Fractions for the Seismic Ground Motion Modeling Case for Commercial SNF Waste Packages (Case 6c Flow Focusing; Results for Seeping Environments Only)

Infiltration Map Percentile[a]	Climate State	Average Rate over the Subregion (m^3/yr per WP)[b]					Repository Average (m^3/yr per waste package)
		1	2	3	4	5	
		0.05 [c]	0.25 [c]	0.4 [c]	0.25 [c]	0.05 [c]	
10 *p*= 0.6191	Present-Day	0.0006	0.0066	0.0114	0.0170	0.0250	0.0117
	Monsoon	0.0053	0.0396	0.0594	0.0780	0.0989	0.0584
	Glacial-Transition	0.0028	0.0241	0.1188	0.3391	0.5453	0.1658
	Post-10,000-year	0.1175	0.7063	1.1280	1.6303	1.6579	1.1241
	Seepage Fraction	0.370	0.446	0.457	0.387	0.452	0.432
30 *p*= 0.1568	Present-Day	0.0050	0.0401	0.0546	0.0715	0.0949	0.0548
	Monsoon	0.0182	0.1178	0.1755	0.2260	0.2602	0.1701
	Glacial-Transition	0.0258	0.1928	0.4372	0.6833	0.8371	0.4371
	Post-10,000-year	0.1056	0.7938	2.1115	3.6698	4.2240	2.1770
	Seepage Fraction	0.394	0.491	0.545	0.514	0.577	0.518
50 *p*= 0.1645	Present-Day	0.0088	0.0770	0.1016	0.1288	0.1828	0.1017
	Monsoon	0.0140	0.1208	0.2394	0.3383	0.4983	0.2362
	Glacial-Transition	0.0190	0.2106	0.6166	1.1048	1.4183	0.6473
	Post-10,000-year	0.1826	1.4537	2.8397	4.2855	4.6456	2.8121
	Seepage Fraction	0.413	0.517	0.552	0.509	0.563	0.526
90 *p*= 0.0596	Present-Day	0.0458	0.3000	0.4213	0.5025	0.5640	0.3996
	Monsoon	0.2272	1.3960	2.1097	2.5214	2.7744	1.9733
	Glacial-Transition	0.0736	0.7371	1.4958	2.0334	2.3809	1.4137
	Post-10,000-year	0.3818	2.0814	3.2015	4.0831	4.2772	3.0547
	Seepage Fraction	0.470	0.570	0.596	0.551	0.601	0.572
TSPA Average Results	Present-Day	0.0053	0.0410	0.0575	0.0729	0.0940	0.0564
	Monsoon	0.0221	0.1465	0.2300	0.2903	0.3500	0.2198
	Glacial-Transition	0.0133	0.1238	0.3326	0.6197	0.8438	0.3618
	Post-10,000-year	0.1421	0.9246	1.6860	2.5306	2.7051	1.6806
	Seepage Fraction	0.387	0.472	0.494	0.436	0.499	0.469

[a] GLUE probability weighting factors for the 10th, 30th, 50th, and 90th percentile infiltration realizations: SAR Section 2.3.2.4.1.2.4.5.5.

[b] Percolation subregions and quantile ranges: SAR Section 2.4.2.3.2.1.2.

[c] Fraction of waste packages in Percolation subregions.

NOTE: TSPA seepage data extracted at 500-, 750-, 10,000-, and 1,000,000-year time steps for the present-day, monsoon, glacial-transition, and post-10,000-year climate states, respectively.

Table 4. Average Seepage Rates and Fractions for the Seismic Ground Motion Modeling Case for Codisposal Waste Packages (Case 6c Flow Focusing; Results for Seeping Environments Only)

Infiltration Map Percentile[a]	Climate State	Average Rate over the Subregion (m^3/yr per WP)[b]					Repository Average (m^3/yr per waste package)
		1	2	3	4	5	
		0.05[c]	0.25[c]	0.4[c]	0.25[c]	0.05[c]	
10 *p*= 0.6191	Present-Day	0.0007	0.0075	0.0139	0.0210	0.0315	0.0143
	Monsoon	0.0057	0.0405	0.0643	0.0824	0.1075	0.0621
	Glacial-Transition	0.0029	0.0241	0.1195	0.3353	0.5522	0.1654
	Post-10,000-year	0.1161	0.7014	1.1390	1.6078	1.6672	1.1221
	Seepage Fraction	0.370	0.445	0.456	0.388	0.450	0.432
30 *p*= 0.1568	Present-Day	0.0069	0.0463	0.0659	0.0845	0.1147	0.0651
	Monsoon	0.0183	0.1243	0.1841	0.2295	0.2711	0.1766
	Glacial-Transition	0.0261	0.1973	0.4362	0.6721	0.8648	0.4363
	Post-10,000-year	0.1075	0.8053	2.1030	3.6238	4.4210	2.1749
	Seepage Fraction	0.399	0.490	0.546	0.513	0.577	0.518
50 *p*= 0.1645	Present-Day	0.0119	0.0832	0.1252	0.1494	0.2136	0.1195
	Monsoon	0.0144	0.1177	0.2437	0.3285	0.5161	0.2356
	Glacial-Transition	0.0187	0.2033	0.6154	1.0514	1.4215	0.6319
	Post-10,000-year	0.1801	1.4352	2.8365	4.1705	4.6579	2.7779
	Seepage Fraction	0.411	0.516	0.553	0.505	0.562	0.525
90 *p*= 0.0596	Present-Day	0.0489	0.3046	0.4750	0.5315	0.6119	0.4320
	Monsoon	0.2135	1.3393	2.1300	2.5521	2.7620	1.9736
	Glacial-Transition	0.0659	0.7075	1.4984	2.0390	2.3594	1.4072
	Post-10,000-year	0.3782	1.9967	3.2107	4.1869	4.1907	3.0586
	Seepage Fraction	0.466	0.567	0.595	0.551	0.597	0.571
TSPA Average Results	Present-Day	0.0064	0.0437	0.0679	0.0826	0.1091	0.0645
	Monsoon	0.0215	0.1442	0.2364	0.2938	0.3591	0.2231
	Glacial-Transition	0.0129	0.1215	0.3329	0.6072	0.8516	0.3585
	Post-10,000-year	0.1409	0.9153	1.6916	2.4969	2.7385	1.6737
	Seepage Fraction	0.387	0.471	0.495	0.436	0.497	0.469

[a] GLUE probability weighting factors for the 10th, 30th, 50th, and 90th percentile infiltration realizations: SAR Section 2.3.2.4.1.2.4.5.5.

[b] Percolation subregions and quantile ranges: SAR Section 2.4.2.3.2.1.2.

[c] Fraction of waste packages in Percolation subregions.

NOTE: TSPA seepage data extracted at 500-, 750-, 10,000-, and 1,000,000-year time steps for the present-day, monsoon, glacial-transition, and post-10,000-year climate states, respectively.

The results for commercial SNF waste packages are very similar to the results for codisposal waste packages with the exception that at early time the codisposal waste packages will cool off sooner than the commercial SNF waste packages. For commercial SNF waste packages, comparing Tables 1 and 3 shows that mean seepage rates for the glacial transition climate state increase by a factor of 3.88 (increase from 0.0932 m^3/yr/WP in Table 1, to 0.3618 m^3/yr/WP in Table 3), with an accompanying decrease in the fraction of waste package locations where seepage occurs (seepage fraction) of 32% from 0.687 to 0.469. The increase in the mean seepage rate for the post-10,000-year results is a factor of 2.51 (based on an increase from 0.6685 m^3/yr/WP to 1.6806 m^3/yr/WP). The increase in seepage rates reflects the influence of the large flow focusing factors at the high end of the distribution for Case 6c (see Figure 1). The decrease in the fraction of waste package locations where seepage occurs (seepage fraction) is consistent with the biasing of flow focusing factors towards lower values in the distribution used for Case 6c (see Figure 1). Similarly, for codisposal waste packages, comparing Tables 2 and 4 shows that mean seepage rates for the glacial transition climate state increase by a factor of 3.87 (increase from 0.0927 m^3/yr/WP in Table 2, to 0.3585 m^3/yr/WP in Table 3), with an accompanying decrease in the seepage fraction of 32%, from 0.687 to 0.469. The increase in the mean seepage rate for the post-10,000-year results is a factor of 2.51 (based on an increase from 0.6677 m^3/yr/WP to 1.6737 m^3/yr/WP).

The smaller seepage fraction that results from using the Case 6c flow focusing distribution, compared to the corrected base case, is shown in Figure 3. This figure compares the average seepage fraction (averaged over aleatory realizations) for each epistemic realization for the Case 6c flow focusing results with the corrected base case. The seepage fractions are uniformly smaller using Case 6c, for nearly all epistemic realizations.

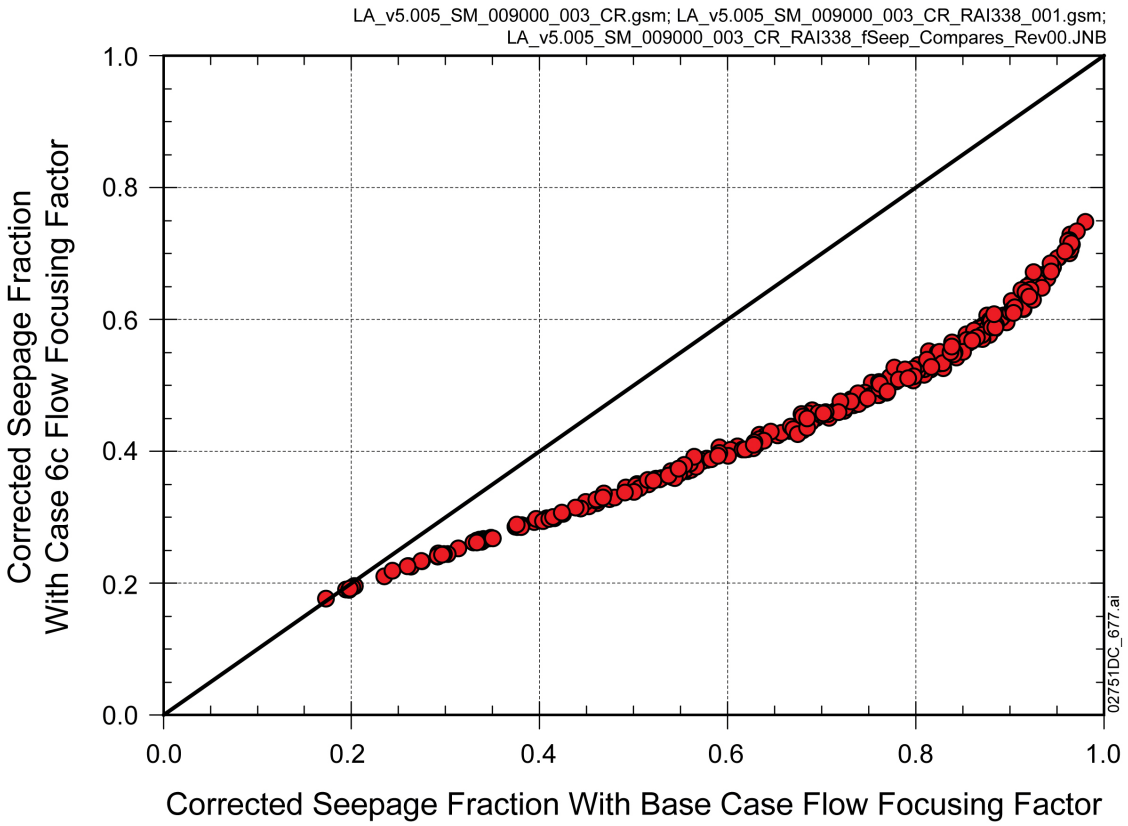

Figure 3. Comparison of Corrected Base Case TSPA Seepage Fraction Results Averaged over Aleatory Realizations, for the 1,000,000-Year Seismic Ground Motion Modeling Case, with Results Using the Case 6c Flow Focusing Factor

Figure 4 compares statistics for the distribution of expected annual dose, for the corrected base case and Case 6c flow focusing distributions, for the 1,000,000-year seismic ground motion modeling case. The effect is relatively small, with an increase in the maximum of the mean annual dose (occurring at 1,000,000 years) of 28% (increase from 1.145 mrem to 1.462 mrem). The slight increase in the maximum of the mean annual dose in the seismic ground motion modeling case at late times (after approximately 700,000 years) results from transport of additional mass of solubility-limited radionuclides such as plutonium, for which the rate of release from the repository is directly related to the increased total seepage flow at all waste package locations. The 95th percentile curve also shows the late-time increase in annual dose, and the median and 5th percentile dose curves show little change.

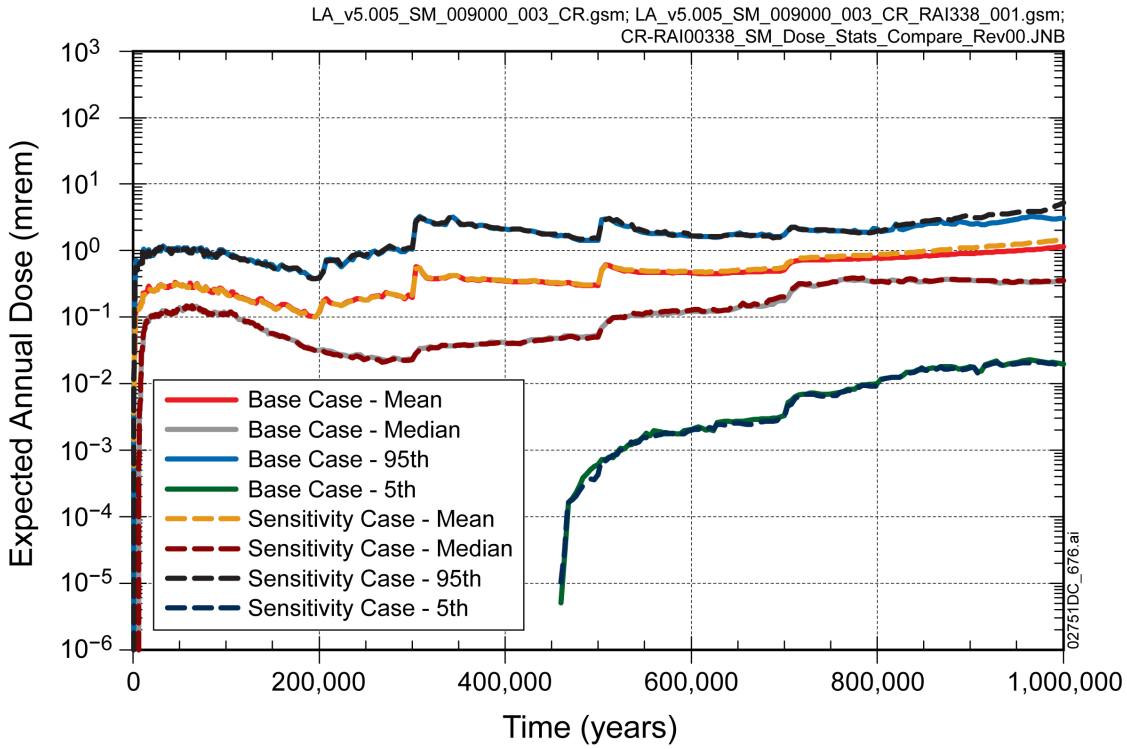

Figure 4. Comparison of Base Case TSPA Mean Annual Dose Results for the 1,000,000-Year Seismic Ground Motion Modeling Case, with Results Using the Case 6c Flow Focusing Factor Distribution

The TSPA sensitivity analysis presented here shows that the performance consequence from using the Case 6c extreme flow focusing distribution is minor. An increase to the total expected annual dose of approximately 0.32 mrem with respect to a base case value of 2.00 mrem (see SNL 2008, Figure 8.1-2[a]) represents a minor effect on performance relative to a regulatory maximum annual dose of 100 mrem, from after 10,000 years, but within the period of geological stability. This result supports the original response to RAI 3.2.2.1.3.6-006, which stated that repository performance is not sensitive to spatial variability in seepage. The unrealistic Case 6c resulted in fewer waste packages experiencing seepage, thus decreasing the seepage fraction compared to the base case (SNL 2007a, Section 6.8.2).

The primary reason for the lack of sensitivity to seepage fraction is the nature of waste package failures in the seismic ground motion modeling case. As presented in the response to RAI 3.2.2.1.4.1-001, in most realizations of the TSPA model, waste package failures in the combined nominal and seismic ground motion modeling case are predominantly from stress-corrosion cracks. In contrast, patch failures by general corrosion, rupture or puncture are observed in only a minority of TSPA model realizations. Consequently, in most realizations, radionuclide transport from failed waste packages is constrained by the rates of diffusion from the waste forms through the waste package and into the invert. These diffusion processes are not significantly sensitive to the presence of seepage, or the rate of seepage, if it occurs. Only when patch failures of waste packages occur is radionuclide transport significantly influenced by changes in seepage fraction or seepage rates. In addition, in the other major case contributing to

dose, the igneous intrusion modeling case, seepage fraction does not play a role after an igneous intrusion occurs. Although the drift seepage abstraction for non-collapsed drifts is used to determine the seepage fraction for placing waste packages into the seeping or non-seeping environments, this placement is only applicable before the igneous intrusion event occurs (see Section 1.4 of the response to RAI 3.2.2.1.3.6-2-010). Prior to the igneous intrusion event, the seepage conditions in the repository are modeled with the drift seepage abstraction for non-collapsed drifts. After the igneous intrusion event has occurred, every waste package location in the repository, whether in a seeping environment or a non-seeping environment, is exposed to dripping (at a rate equal to the product of the percolation rate and the effective area of the waste package) and the applicable abstractions for seeping conditions in the emplacement drifts are applied in both the seeping and non-seeping environments. This is modeled by applying dripping specific calculations (e.g., the liquid influx in-package chemistry abstraction) instead of non-dripping specific calculations (e.g., the vapor influx in-package chemistry abstraction), and by not reassigning waste packages between seeping and non-seeping groups.

2. COMMITMENTS TO NRC

None.

3. DESCRIPTION OF PROPOSED LA CHANGE

None.

4. REFERENCES

BSC (Bechtel SAIC Company) 2004. *Conceptual Model and Numerical Approaches for Unsaturated Zone Flow and Transport.* MDL-NBS-HS-000005 REV 01. Las Vegas, Nevada: Bechtel SAIC Company. ACC: DOC.20040922.0006; DOC.20050307.0009.

SNL (Sandia National Laboratories) 2007a. *Abstraction of Drift Seepage*. MDL-NBS-HS-000019 REV 01 AD 01. Las Vegas, Nevada: Sandia National Laboratories. ACC: DOC.20070807.0001; DOC.20080813.0004; DOC.20081118.0049[a].

SNL 2007b. *Calibrated Unsaturated Zone Properties*. ANL-NBS-HS-000058 REV 00. Las Vegas, Nevada: Sandia National Laboratories. ACC: DOC.20070530.0013; DOC.20070713.0005; LLR.20080423.0015; LLR.20080527.0082.

SNL 2008. *Total System Performance Assessment Model /Analysis for the License Application*. MDL-WIS-PA-000005 REV 00 AD 01. Las Vegas, Nevada: Sandia National Laboratories. ACC: DOC.20080312.0001; LLR.20080414.0037; LLR.20080507.0002; LLR.20080522.0113; DOC.20080724.0005.

NOTE: [a]Provided as an enclosure to letter from Williams to Sulima dtd 02/17/2009. "Yucca Mountain – Request for Additional Information Re: License Application (Safety Analysis Report Section 2.1), Safety Evaluation Report Volume 3 – Postclosure Chapters 2.2.1.1 and 2.2.1.3.7 – Submittal of Department of Energy Reference Citations."

APPENDIX A

DERIVATION OF EQUATION 1

The base case flow focusing distribution is

$$Y = AX^4 + BX^3 + CX^2 + DX + E \qquad \text{(Eq. A-1)}$$

Where

$A = -0.3137$

$B = 5.4998$

$C = -35.66$

$D = 102.3$

$E = -11.434$

$X \equiv$ flow focusing factor

$Y \equiv$ cumulative probability percentage

(SNL 2007a, p. 6.6-15)

The range of X for the base case distribution is from 0.116 to 5.016 (SNL 2007a, p. 6-154)

The alternative distribution uses the following change in variables,

$$Z = X^3 \qquad \text{(Eq. A-2)}$$

where Z is the unnormalized alternative flow focusing factor. Substituting Equation A-2 into Equation A-1 gives,

$$Y = AZ^{4/3} + BZ + CZ^{2/3} + DZ^{1/3} + E \qquad \text{(Eq. A-3)}$$

The mean flow focusing factor is developed from the probability density function,

$$\frac{dY}{dZ} = \frac{4}{3}AZ^{1/3} + B + \frac{2}{3}CZ^{-1/3} + \frac{1}{3}DZ^{-2/3} \qquad \text{(Eq. A-4)}$$

$$Z_{mean} = \frac{1}{100}\int_{Z_{min}}^{Z_{max}} Z\frac{dY}{dZ}dZ \qquad \text{(Eq. A-5)}$$

Substituting Equation A-4 into A-5 gives,

$$Z_{mean} = \left(\frac{4}{7}AZ^{7/3} + \frac{1}{2}BZ^2 + \frac{2}{5}CZ^{5/3} + \frac{1}{4}DZ^{4/3}\right)\Big|_{Z_{min}}^{Z_{max}} \qquad \text{(Eq. A-6)}$$

Evaluating for $Z_{max} = (5.016)^3 = 126.2$ and $Z_{min} = (0.116)^3 = 0.001561$ gives

$$Z_{mean} = 3.748 \qquad \text{(Eq. A-7)}$$

Therefore, the normalized alternative flow focusing distribution is,

$$Z_n = Z/Z_{mean} \qquad \text{(Eq. A-8)}$$

$$Y = AZ_{mean}{}^{4/3}Z_n^{4/3} + BZ_{mean}Z_n + CZ_{mean}{}^{2/3}Z_n{}^{2/3} + DZ_{mean}{}^{1/3}Z_n{}^{1/3} + E \qquad \text{(Eq. A-9)}$$

Numerically, this is,

$$Y = -1.826Z_n{}^{4/3} + 20.61Z_n - 86.04Z_n{}^{2/3} + 158.9Z_n{}^{1/3} - 11.434 \qquad \text{(Eq. A-10)}$$

A value of $Z_n = 33$ gives a cumulative probability percentage, $Y = 99.95$. Equation A-10 is equivalent to Equation 1 in the main text.